International Journal of Thermophysics, Vol. 25, No. 4, July 2004 (© 2004)

Effects of Concentration on Steady-State Viscometric Properties of Short Chain Polymer Solutions Over the Entire Concentration Range[1]

T. Kairn,[2] P. J. Daivis,[2,3] M. L. Matin,[2] and I. K. Snook[2]

Relationships between viscometric behavior and concentration are observed and evaluated through a series of nonequilibrium molecular dynamics simulations of the behavior of 20-site polymers in solution with explicit solvent across the full concentration range. The zero-shear viscosities, first normal stress coefficients and steady-state shear compliance of the solutions are examined alongside conformational properties including the excluded volume effect. The variation of viscosity with concentration in these solutions is described by the Huggins equation up to relatively high concentrations. At these high concentrations, the effects on conformation of excluded volume interactions decline, while no clear semi-dilute region is identifiable. Although the steady-state shear compliance of the system appears concentration-independent, the dilute and melt behaviors of this system are accurately described by the theories of Zimm and Rouse, respectively.

KEY WORDS: bead-rod model polymer; nonequilibrium molecular dynamics; polymer solution; shear flow; viscosity.

1. INTRODUCTION

This study examines the viscometric properties of short polymer chains in solution through a series of nonequilibrium molecular dynamics (NEMD) simulations. The viscometric and conformational properties of short-chain

[1]Paper presented at the Fifteenth Symposium on Thermophysical Properties, June 22–27, 2003, Boulder, Colorado, U.S.A.

[2]Department of Applied Physics, RMIT University, GPO Box 2476V, Melbourne, Victoria 3001, Australia

[3]To whom correspondence should be addressed. E-mail: peter.daivis@rmit.edu.au

0195-928X/04/0700-1075/0

polymer solutions are of importance to a range of polymer science applications, including lubrication technology.

Simulation-based analyses of viscometric properties have been previously undertaken using a system containing a single polymer molecule, where "concentration" throughout the periodic system is determined according to the number of solvent molecules in the periodic box [1–3]. In this study, NEMD simulations are completed on systems of 100–500 chain molecules. The polymer molecules themselves have $N = 20$ interaction sites, and are suspended in a solvent of single-site molecules, so that polymer concentration can be modified by altering the percentage of sites within the simulation box which are constrained to form chains. In terms of their conformational behavior, we have previously demonstrated [4] that these $N = 20$ chains can be regarded as approximately modeling real polyethylene oligomers approximately 128 repeat units long, with molar mass $M \simeq 1800\,\mathrm{g{\cdot}mol^{-1}}$.

Since our simulations are performed at a range of very low homogeneous shear rates, the zero-shear-rate viscosity, η, can be easily identified for each concentration. Charting the changes in η as polymer concentration increases allows us to test the theories of chain behavior.

With the exception of Ref. 4, the current authors are unaware of any other computational or experimental study of polymers which examines viscometric and conformational behavior over the entire concentration range. The fragmentary nature of many experimental studies of viscosity and concentration mirrors the disjointedness of the relevant theory. Separate relations exist to describe viscosity behavior in the dilute, semi-dilute, and concentrated regimes. The aim of the current study is to examine the relationships between viscosity, conformation, and concentration exhibited by a short-chain polymer solution, with reference to some of the various theoretical models available.

2. MOLECULAR MODEL AND SIMULATION TECHNIQUE

The simulation technique used to achieve the results described in Section 3 has been reported previously [4]. We use a NEMD code (described by Matin et al. [5]) which explicitly applies the molecular version of the SLLOD equations of motion (given in Refs. 4 and 5) to all particles in the system, including those comprising the solvent and solves these equations at each time-step by a fourth-order Gear predictor–corrector scheme. The solvent molecules are modeled as Lennard–Jones (LJ) spherical particles, while the polymer molecules are made up of 20-site chains of identical spheres. These chains are simulated according to a bead-rod model with truncated and shifted LJ interactions between all beads ('sites') except

those which are bonded to each other within a molecule. The LJ potential describing all interactions in the system is truncated and shifted so that the potential has no discontinuity and is zero beyond a cutoff distance $r_c = 2^{1/6}\sigma$ (where σ is the distance at which the unshifted potential is zero). An LJ potential with this truncation point is often known as the WCA potential [6], and it results in purely repulsive interactions. This potential is convenient for computational work because it is short-ranged, and therefore computationally undemanding, but still retains the essential physics, i.e., the repulsive (excluded volume) interaction.

The molecular center of mass temperature for the polymer chains (defined as proportional to the square of the center of mass momentum of each chain divided by its molecular mass, per number of translational center of mass degrees of freedom available to the molecules) is kept constant through the inclusion of a thermostatting term derived from Gauss' principle of least constraint. This algorithm, including the details of the constraint algorithm, has been discussed previously [7–9] and we refer the reader to previous work [10–13] on the subtle but important issues involved in the application of homogeneous thermostats to flowing molecular fluids.

Bulk behavior of this system simulated via periodic boundary conditions (PBCs) and the minimum image convention, which prescribes that the primary simulation box must be large enough so that each particle interacts only with the closest image of another particle [14]. Here, to allow for the homogeneous shear flow introduced to the system via the equations of motion, we apply Lagrangian rhomboid periodic boundary conditions, where periodic images are deformed in the x direction by an amount dependent on their location in the y direction. These effects result in a velocity gradient in the y-direction which, when the fluid state is at equilibrium and the flow rate is not too great [15], is equivalent to planar shear flow $\dot{\gamma} = \partial v_x / \partial y$. This method is periodic in space and time, allowing shear flow of an infinite bulk system to be simulated over very many time-steps.

The viscometric functions under consideration in this study are defined in terms of components of the pressure tensor $\mathbf{P}$. The pressure tensor for the atomic fluid (single interaction site molecules) was calculated using the atomic pressure tensor, given by

$$\boldsymbol{P}_A V = \left\langle \sum_{i=1}^{N_a} \frac{\boldsymbol{p}_i \boldsymbol{p}_i}{M_i} - \frac{1}{2} \sum_{i=1}^{N_a} \sum_{j \neq i}^{N_a} \boldsymbol{r}_{ij} \boldsymbol{F}_{ij} \right\rangle, \tag{1}$$

while for the polymer solutions, it was calculated using the expression

$$\boldsymbol{P}_M V = \left\langle \sum_{i=1}^{N_m} \frac{\boldsymbol{p}_i \boldsymbol{p}_i}{M_i} - \frac{1}{2} \sum_{i=1}^{N_m} \sum_{\alpha=1}^{N} \sum_{j \neq i}^{N_m} \sum_{\beta=1}^{N} \boldsymbol{r}_{ij} \boldsymbol{F}_{i\alpha j\beta}^{\text{inter}} \right\rangle, \tag{2}$$

where $\mathbf{p}_i$ represents the total peculiar momentum of molecule i, as defined by the equations of motion, and $\boldsymbol{F}_{i\alpha j\beta}^{\text{inter}}$ represents the intermolecular force on site $i\alpha$ due to site $j\beta$. This means that the first term in each equation represents the kinetic component while the second describes the potential component of the pressure tensor.

For simple shear flow, η_s and Ψ_1 are useful material functions for representing and relating independent components of the stress tensor. η_s is the generalized non-Newtonian shear viscosity of a fluid subject to strain rate $\dot{\gamma}$ and is defined by

$$\eta_s = -\frac{\boldsymbol{P}_{xy} + \boldsymbol{P}_{yx}}{2\dot{\gamma}}. \tag{3}$$

Ψ_1 is the first normal stress coefficient, given by the first two diagonal components of $\boldsymbol{P}$,

$$\Psi_1 = \frac{\boldsymbol{P}_{yy} - \boldsymbol{P}_{xx}}{\dot{\gamma}^2} = \frac{N_1}{\dot{\gamma}^2}. \tag{4}$$

It is related to the first normal stress difference, N_1, which results directly from restoring forces acting in opposition to any flow-induced anisotropy in the fluid.

A general relationship linking the steady-state values of η_s and Ψ_1 for rheologically simple fluids has been identified by Ferry [16];

$$\Psi_{1,0} = 2\eta^2 J_e^0. \tag{5}$$

Here J_e^0 is the steady-state shear compliance of the fluid, which can also be calculated from η the steady-state viscosity of the solution, η_0 the solvent viscosity, S_2/S_1^2 the relaxation-time ratio, and n_1 the polymer concentration, according to

$$J_e^0 = \left(\frac{M}{n_1 RT} \right) \frac{(\eta - \eta_0)^2}{\eta^2} \frac{S_2}{S_1^2}, \tag{6}$$

where R is the universal gas constant, M is the polymer molar mass, and T is the absolute temperature. This general relationship for polymer solutions can be applied to dilute solutions where Zimm theory includes hydrodynamic solvent interactions when calculating the total force on each

polymer site and predicts that $S_2/S_1^2 = 0.206$. Alternately, in the high-concentration limit, Rouse theory predicts that $S_2/S_1^2 = 0.400$, where solvent-mediated hydrodynamic interactions between polymer sites are ignored [16].

These relationships have been shown to apply to simulations of a very short polymer chains, like those used here. For example, Matin [14] has shown that polymers with length $N = 20$ in a melt are flexible enough to exhibit a chain-length-dependent viscosity consistent with Rouse theory. Furthermore, the applicability of the Zimm model to dilute solutions of short-chain polymers has been demonstrated by Dunweg and Kremer [17], down to $N = 30$. We can therefore be confident that our short chains are accurately simulating real polymers, and that the theoretical relationships derived from polymer rheology should predict their behavior.

3. RESULTS AND DISCUSSION

In the remainder of this paper, we express all quantities in terms of site reduced units for which the reduction parameters are the LJ interaction parameters ε and σ and the mass $m_{i\alpha}$ of site α on molecule i. These values are defined in terms of reduced temperature $T^* = k_B T/\varepsilon = 1.0$, reduced density $\rho^* = \rho\sigma^3 = 0.84$, and the mass of each site $m^* = m_{i\alpha} = 1.0$, while time is scaled by $t^* = \sigma m^{1/2}\varepsilon^{-1/2}t$. The asterisk denoting reduced quantities will be omitted from here on.

The parameter n_1 defines polymer site fraction, the proportion of interaction sites in the system that belong to polymer molecules, and is used henceforward to describe the concentration of the systems. Table I lists the n_1 values used in this study.

The shear rates used in these simulations were $\dot{\gamma} = 0.0000$, 0.0005, 0.00071, 0.0010, 0.0016, and 0.0022. MD simulations of polymer solutions usually use shear rates of between $\dot{\gamma} = 0.01$ and $\dot{\gamma} = 10$ (see, for example, Refs. 18 and 19). Here we use relatively low $\dot{\gamma}$ values, which fall within the range of shear rates accessible to current experiments [20], so that changes in the pressure of the system with shear rate are negligible. A further advantage of using these low values is that the solutions persist in Newtonian behavior over almost all shear rates allowing zero-shear-rate viscosities to be very easily extrapolated.

The zero-shear-rate viscosity results shown in Table I were obtained via linear extrapolation to $\dot{\gamma}^2 = 0$ (using a weighted least-squares fit) of our η_s vs $\dot{\gamma}^2$ data (illustrated in Ref. 4). It is evident from these results that the zero shear rate viscosity (η) increases with increasing polymer

Table I. Simulation Parameters and Viscosity Data. (Total number of sites (N_s), number of polymer molecules (N_m), and polymer site fraction (n_1) alongside limiting first normal stress coefficient ($\Psi_{1,0}$), zero shear rate viscosity (η), and relaxation-time ratio (S_2/S_1^2) results.)

N_s	N_m	n_1	$\Psi_{1,0} \times 10^{-2}$	η	S_2/S_1^2
10000	000	0.0	-0.3 ± 0.8	1.8 ± 0.1	
10000	100	0.2	-0.6 ± 0.4	4.03 ± 0.7	-0.06 ± 0.03
10000	200	0.4	5.5 ± 0.9	5.60 ± 0.9	0.38 ± 0.09
10000	300	0.6	7.8 ± 0.7	8.2 ± 0.1	0.28 ± 0.04
10000	400	0.8	15.0 ± 0.8	11.3 ± 0.1	0.33 ± 0.03
10000	500	1.0	33 ± 2	16.0 ± 0.3	0.45 ± 0.05

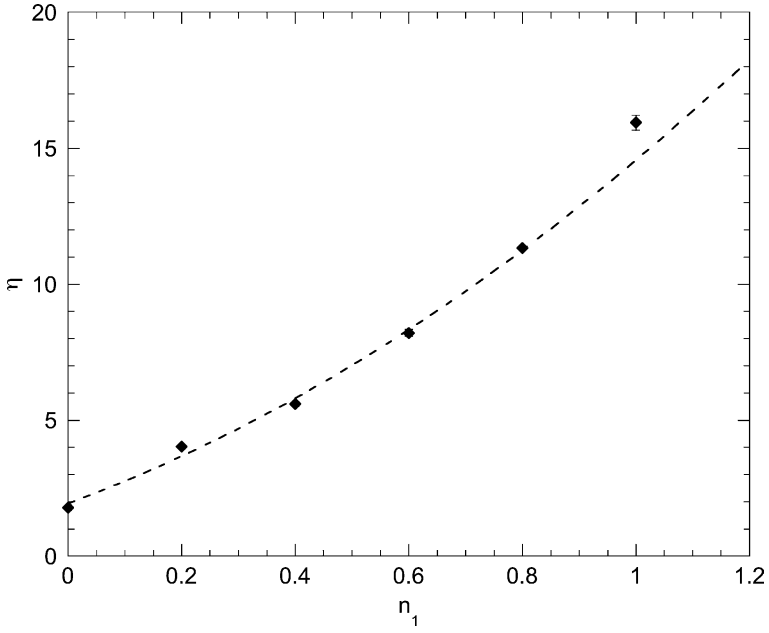

Fig. 1. Zero shear viscosity, η, versus polymer concentration, n_1, showing second-order polynomial fit to all data points except $n_1 = 1.0$ (horizontal axis extends to unphysical value of $n_1 = 1.2$ for clarity only).

concentration (n_1). These data are shown in Fig. 1, where they are fitted by a polynomial that obeys the Huggins equation,

$$\eta = \eta_0 \left(1 + [\eta] n_1 + k_H [\eta]^2 n_1^2 + \cdots\right), \tag{7}$$

where the Huggins constant k_H is 0.16 ± 0.04 and the intrinsic viscosity of the polymer in this very good solvent is $[\eta] = 4.0 \pm 0.4$. This relationship is expected to hold only for low-concentration polymer solutions. However, our results show a persistence of dilute-like behavior over a much broader concentration range.

Our study of the conformation of this system [4] confirms this observation in that the polymer molecules in the system exhibit a strong excluded volume effect, up to relatively high concentrations. The mean-field theory predicts that polymer solutions will exhibit an increasing degree of excluded volume screening as polymer concentration is increased, with excluded volume interactions disappearing in concentrated solutions, whereas the scaling theory predicts that Gaussian behavior, with its obviation of long-range interactions, should be seen at lower, semi-dilute concentrations [21]. While our previously reported conformation results show the expected decline in excluded volume interactions over high concentrations (greater than $n_1 = 0.4$), it is not until the $n_1 = 1.0$ melt is reached that the polymers in the system begin to display ideal Gaussian behavior. For our very short polymer chains, there is no clear transition into a semi-dilute regime as predicted by scaling theory.

As a further exploration of the behavior of this system, the limiting values of the first normal stress coefficient $\Psi_{1,0}$ are examined at each concentration. These values, listed in Table I, are calculated as the gradients of weighted linear fits to the shear-dependent N_1 data (illustrated in Ref. 4), which is linear over the low-shear region simulated. Figure 2 shows the value of $\Psi_{1,0}$ at each concentration plotted against $2\eta^2$, a multiple of the zero-shear viscosity of each solution. Relating Eq. (5) to the gradient shown in this figure leads to the conclusion that the steady-state shear compliance of the fluid remains constant at $J_e^0 = \Psi_{1,0}/(2\eta^2) = 6.8 \pm 0.3$ and does not appreciably vary with concentration. That J_e^0 may be constant with respect to concentration, for very short polymer chains, is implied by the results of Holmes and Ferry [23]. In their experimental study of polystyrene molecules suspended in aroclors (chlorinated biphenyls), they note that J_e^0 goes through a maximum as the concentration is increased and that this maximum shifts to higher concentrations as the molar mass of the polystyrene is reduced. However, it is also clear from their results that the height of this steady-state shear compliance maximum decreases with decreasing polystyrene molar mass; J_e^0 becomes more constant as the polymer chains are shortened. Holmes and Ferry achieve reliable results displaying a slight peak in J_e^0 for polystyrene polymers as short as $M = 82{,}000\ \mathrm{g \cdot mol^{-1}}$. We therefore conclude that the trends in their results are compatible with the observation that J_e^0 is constant for very short, $M = 1800\ \mathrm{g \cdot mol^{-1}}$, polyethylene.

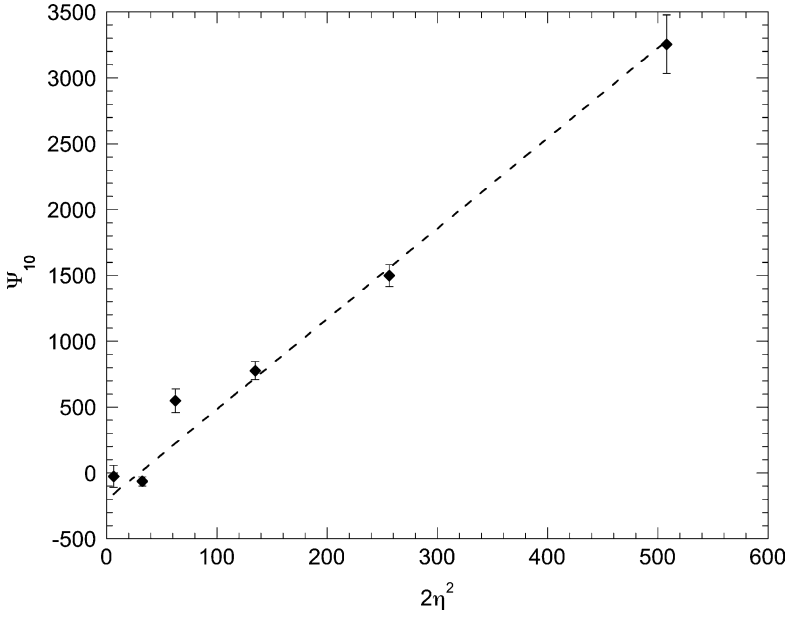

Fig. 2. Limiting first normal stress coefficient $\Psi_{1,0}$ versus $2\eta^2$ (horizontal error bars are smaller than plot symbols).

The constancy of J_e^0 contrasts with the behavior of J_{eR}^0, the reduced steady-state shear compliance, which is regarded as being equivalent to S_2/S_1^2, the relaxation-time ratio of the fluid. Combining Eqs. (5) and (6) results in

$$J_{eR}^0 = \frac{\Psi_{1,0} n_1 RT}{2M(\eta - \eta_0)^2} = \frac{S_2}{S_1^2}.$$

Here, the ratio of relaxation times, S_2/S_1^2, represents the degree of hydrodynamic interaction in the system. As noted in Section 2, Zimm theory predicts a value of $S_2/S_1^2 = 0.206$ for low-concentration systems, whereas Rouse theory predicts that $S_2/S_1^2 = 0.400$, in the high-concentration limit.

In Fig. 3, these values are plotted against $n_1[\eta]$, where they are expected to form a universal curve, independent of molar mass, as exemplified by the data of Holmes and Ferry [22]. It is clear that, while the result for the $n_1 = 0.2$ system falls below the expected minimum of 0.206, S_2/S_1^2 values generally trend towards the Rouse prediction, for high concentrations.

The change from Zimm-like to Rouse-like behavior with increasing polymer concentration signifies a transition from a hydrodynamically inter-

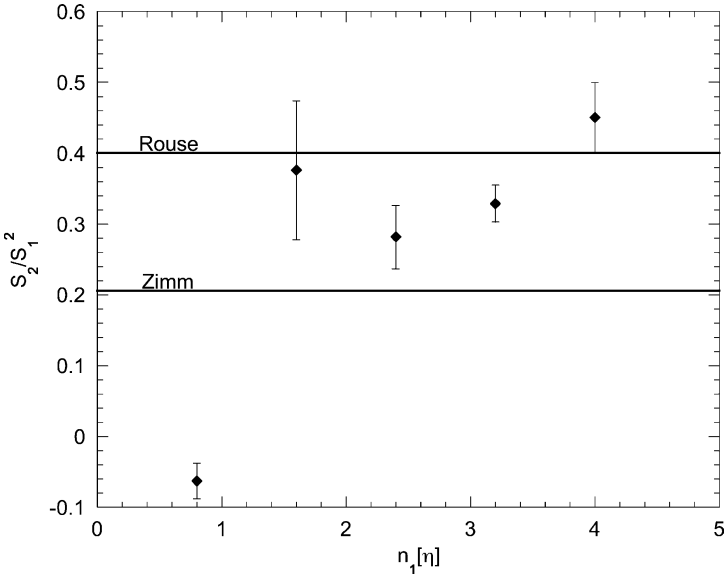

Fig. 3. Ratio of relaxation times (S_2/S_1^2) versus concentration, showing Rouse ($S_2/S_1^2 = 0.400$) and Zimm ($S_2/S_1^2 = 0.206$) values.

acting regime to a concentrated regime with no apparent hydrodynamic interactions.

4. CONCLUSION

Here, we have examined the behavior of $N = 20$ WCA polymer molecules solvated by a LJ fluid, over the entire concentration range. This system models a solution of short chains of polyethylene, with $M \simeq 1800\,\mathrm{g \cdot mol^{-1}}$.

The effects on solution behavior of using a very short polymer and a very good solvent can be clearly seen in the persistent adherence of the viscosities to Huggins' prediction, which suggests that the polymers exhibit dilute-like behavior over a broad range of concentrations.

While the steady-state shear compliance remains constant, the system examined here shows a clear trend from Zimm-like to Rouse-like behaviors as the concentration is increased, indicating that hydrodynamic interactions decrease according to expectations.

Similarly, the expected waning of the excluded volume effect can be observed in the system at high concentrations. However, for these short chains, the onset of the concentrated regime is not preceded by the rec-

ognizable crossover from dilute to semi-dilute solution behavior predicted by the scaling or mean-field polymer theories.

These results demonstrate that solutions of short-chain polymers, while seemingly conforming to a range of predictable behaviors, can nonetheless challenge the limits of accepted theoretical approaches.

ACKNOWLEDGMENTS

This work was supported by the Cooperative Research Center for MicroTechnology and through an Expertise Grant from the Victorian Partnership for Advanced Computing. We would like to thank the CSIRO/ Bureau of Meteorology High Performance Computing and Communications Center and the Australian and Victorian Partnerships for Advanced Computing for generous allocations of computer time.

REFERENCES

1. C. Pierleoni and J.-P. Ryckaert, *J. Chem. Phys*. **113**:5545 (2000).
2. Y. N. Kaznessis, D. A. Hill, and E. J. Maginn, *J. Chem. Phys*. **109**:5078 (1998).
3. I. Bahar, B. Badur, and P. Doruker, *J. Chem. Phys*. **99**:2235 (1993).
4. T. Kairn, P. J. Daivis, M. L. Matin, and I. K. Snook, *Polymer* **45**:2453 (2004).
5. M. L. Matin, P. J. Daivis, and B. D. Todd, *J. Chem. Phys*. **113**:9122 (2000); Erratum: M. L. Matin, P. J. Daivis, and B. D. Todd, *J. Chem. Phys*. **115**:5338 (2001).
6. J. D. Weeks, D. Chandler, and H. C. Andersen, *J. Chem. Phys*. **54**:5237 (1971).
7. R. Edberg, D. J. Evans, and G. P. Morriss, *J. Chem. Phys*. **84**:6933 (1986).
8. R. Edberg, G. P. Morriss, and D. J. Evans, *J. Chem. Phys*. **86**:4555 (1987).
9. G. P. Morriss and D. J. Evans, *Comput. Phys. Commun*. **62**:267 (1991).
10. K. P. Travis, P. J. Daivis, and D. J. Evans, *J. Chem. Phys*. **103**:1109 (1995).
11. K. P. Travis, P. J. Daivis, and D. J. Evans, *J. Chem. Phys*. **103**:10638 (1995). Erratum: K. P. Travis, P. J. Daivis, and D. J. Evans, *J. Chem. Phys*. **105**:3893 (1996).
12. K. P. Travis and D. J. Evans, *Mol. Sim*. **17**:157 (1996).
13. P. Padilla and S. Toxvaerd, *J. Chem. Phys*. **104**:5956 (1996).
14. M. L. Matin, *Molecular Simulation of Polymer Rheology*, Ph. D. Thesis, Applied Physics, RMIT University, Melbourne (2001).
15. S. Hess, *Int. J. Thermophys*. **23**:905 (2002).
16. J. D. Ferry, *Viscoelastic Properties of Polymers* (John Wiley, New York, 1980).
17. B. Dunweg and K. Kremer, *Phys. Rev. Lett*. **66**:2996 (1991).
18. W. Brostow and M. Drewniak, *J. Chem. Phys*. **105**:7135 (1996).
19. S. Hess, C. Aust, L. Bennett, M. Kroeger, C. Pereira Borgmeyer, and T. Weider, *Physica A* **240**:126 (1997).
20. S. Bair, C. McCabe, and P. T. Cummings, *Phys. Rev. Lett*. **88**:088302/1 (2002).
21. M. Doi and S. F. Edwards, *The Theory of Polymer Dynamics* (Clarendon Press, Oxford, 1986).
22. L. A. Holmes and J. D. Ferry, *J. Polym. Sci.: Part C*. **23**:291 (1968).